

# Influence of postdeposition annealing on the properties of Ga<sub>2</sub>O<sub>3</sub> films on SiO<sub>2</sub> substrates

Hyoun Woo Kim\*, Nam Ho Kim

*School of Materials Science and Engineering, Inha University, Incheon 402-751, Korea*

Received 7 January 2004; accepted 20 May 2004

## Abstract

We have investigated the structural and optical properties of annealed gallium oxide (Ga<sub>2</sub>O<sub>3</sub>) film in the range of 750–1050 °C, which had been grown on SiO<sub>2</sub> substrates by the metal organic chemical vapor deposition (MOCVD) technique. We revealed that postdeposition annealing of amorphous Ga<sub>2</sub>O<sub>3</sub> generated grains in β-Ga<sub>2</sub>O<sub>3</sub> phase. While photoluminescence spectra of as-deposited Ga<sub>2</sub>O<sub>3</sub> films showed strong blue–green (BG) and ultraviolet (UV) emission, postdeposition annealing at high temperatures resulted in appearance of a longer wavelength UV band and a new green band.

© 2004 Elsevier B.V. All rights reserved.

PACS: 81.15Gh; 68.55Jk

Keywords: Thin films; Chemical synthesis; X-ray diffraction; Luminescence

## 1. Introduction

Since metal oxides exist in a variety of compositions and crystal structures and their property vary widely from insulators to superconductors, metal oxide thin films are finding rapidly growing applications in advanced technologies. Especially, gallium oxide (Ga<sub>2</sub>O<sub>3</sub>) crystals have recently attracted considerable attention as materials for the new generation of optoelectronic devices [1–5], since the crystals are transparent in a wide range of ultraviolet (UV) down to 280 nm and they are potentially electro-conductive. These characteristics originate from their band gaps of about 4.8 eV and n-type conductivity. Additionally, Ga<sub>2</sub>O<sub>3</sub> has been considered as one of the most promising materials as a metal oxide gas sensor [6–8], due to its n-type semiconductor property and its stability in the high temperature range over 600 °C [9].

Although various techniques have been employed to prepare the Ga<sub>2</sub>O<sub>3</sub> films [10–18], metal organic chemical vapor

deposition (MOCVD) method offers more flexible approach to the growth of metal oxides. Additionally, this method has several other advantages of producing uniform, pure, reproducible, adherent, and good step-coverage films. In spite of their several advantages, there are only few reports on the growth of Ga<sub>2</sub>O<sub>3</sub> thin films by the MOCVD techniques and the precursors of Ga(hfac)<sub>3</sub>, Ga[OCH(CF<sub>3</sub>)<sub>2</sub>]<sub>3</sub>•HNMe<sub>2</sub>, [Ga(μ-O-t-Bu)(O-t-Bu)<sub>2</sub>]<sub>2</sub> and Ga(O<sup>*i*</sup>Pr)<sub>3</sub> have been investigated [19–22].

In the present work, we have deposited the Ga<sub>2</sub>O<sub>3</sub> thin films on SiO<sub>2</sub> substrates at a temperature of 550 °C, using a conventional precursor of trimethylgallium (TMGa). With an expectation of transforming Ga<sub>2</sub>O<sub>3</sub> films to its stable β-phase, we have annealed the Ga<sub>2</sub>O<sub>3</sub> thin films at temperatures in the range of 750–1050 °C and have investigated the effect of annealing on the structural properties of Ga<sub>2</sub>O<sub>3</sub> thin films, by comparing the annealed films to the as-grown films, using scanning electron microscopy (SEM), X-ray diffraction analysis (XRD), and atomic force microscopy (AFM). We also have studied the optical properties of the as-deposited and annealed Ga<sub>2</sub>O<sub>3</sub> films using room temperature photoluminescence (PL).

\* Corresponding author. Tel.: +82 32 860 7544; fax: +82 32 862 5546.  
E-mail address: hwkim@inha.ac.kr (H.W. Kim).

## 2. Experimental

The  $\text{Ga}_2\text{O}_3$  films were deposited on  $\text{SiO}_2$  substrates, which were prepared by depositing a 60-nm-thick  $\text{SiO}_2$  layer on  $\text{Si}(1\ 0\ 0)$  substrate thermally. The substrate was cleaned in acetone for 10 min, in HF (20:1) for 1 min and then rinsed in deionized water for 1 min before loading into the system. A schematic diagram of the MOCVD system used in this experiment is described in Fig. 1. TMGa and  $\text{O}_2$  were used as sources. High-purity Ar passed through the TMGa bubbler, which had been maintained at the temperature of  $-5\text{ }^\circ\text{C}$ , and delivered the TMGa vapor to the reactor. The  $\text{Ga}_2\text{O}_3$  film was synthesized by supplying  $\text{O}_2$  and Ar carrier gases with the flow rate of 30 standard cubic centimeters per min (sccm) and 30 sccm, and the reaction temperature was set to  $550\text{ }^\circ\text{C}$ . Thermal annealing after the growth was done in air ambient for 1 h. The annealing temperatures were varied between  $700$  and  $1050\text{ }^\circ\text{C}$ .

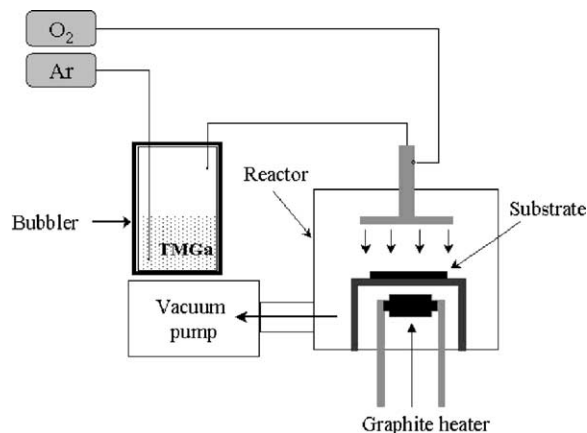


Fig. 1. Schematic illustration of the MOCVD reactor.

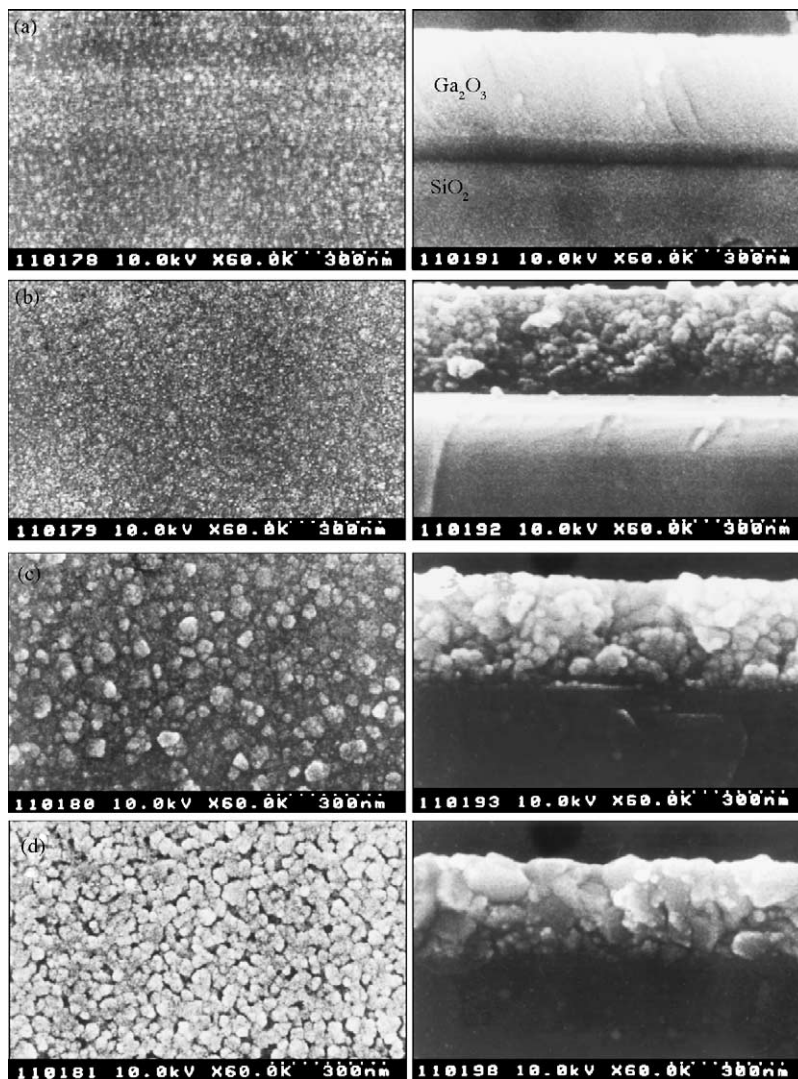


Fig. 2. Plain-view SEM images (left: plain-view images, right: cross-sectional images) of (a) as-deposited, (b)  $750\text{ }^\circ\text{C}$ -annealed, (c)  $900\text{ }^\circ\text{C}$ -annealed, and (d)  $1050\text{ }^\circ\text{C}$ -annealed  $\text{Ga}_2\text{O}_3$  thin films.

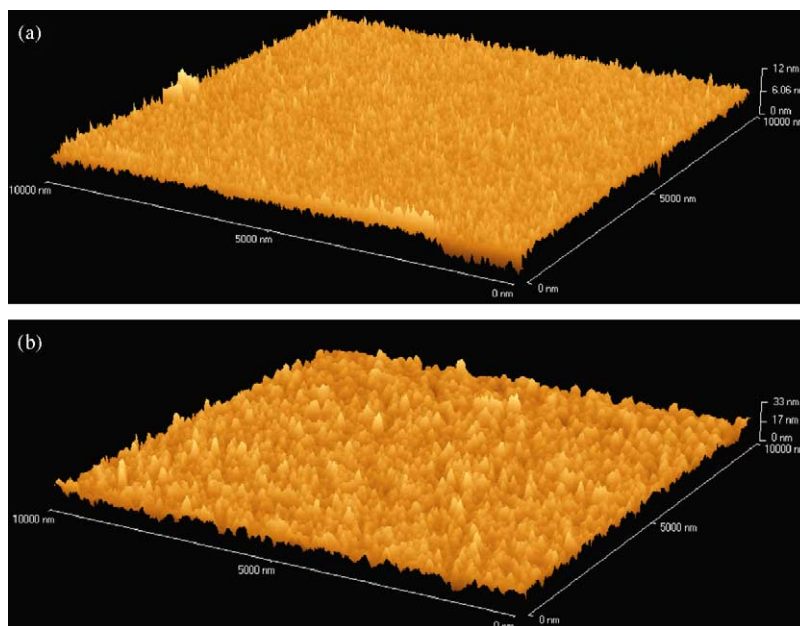


Fig. 3. AFM images of (a) as-deposited and (b) 1050 °C-annealed Ga<sub>2</sub>O<sub>3</sub> thin films.

The structural characteristics of the films were analyzed by XRD (Philips, CM20T, 200 kV) using Cu K $\alpha$ 1 radiation ( $\lambda = 0.154056$  nm) and SEM (Hitachi S-4200). The surface roughness was measured by using an AFM (Nanoscope III, Digital Instruments) with a scan size of 10  $\mu\text{m} \times 10 \mu\text{m}$ . PL measurements were carried out at room temperature with a Shimadzu fluorescence spectrophotometer (RF-5301PC). The excitation light was the monochromatic light from a xenon short arc lamp with a wavelength of  $\lambda = 250$  nm.

### 3. Results and discussion

Fig. 2a–d show the SEM images of Ga<sub>2</sub>O<sub>3</sub> thin films, respectively, which are as-deposited, 750 °C-annealed, 900 °C-annealed, and 1050 °C-annealed. Plain-view SEM images indicate that by the thermal annealing process at 900–1050 °C, the microstructure tends to change into the grain-like structures. The cross-sectional SEM images also indicate that although no clear grain boundaries are found inside the as-grown Ga<sub>2</sub>O<sub>3</sub> thin films, the grain-like structure appears by the thermal annealing. Furthermore, the size of the grain-like structure becomes larger with increasing the annealing temperature in the range of 900–1050 °C.

In order to investigate the surface roughness of the Ga<sub>2</sub>O<sub>3</sub> films grown on SiO<sub>2</sub> substrates, we have performed an AFM analysis. Fig. 3a and b show the AFM topographies representing the surface morphology of as-deposited and 1050 °C-annealed Ga<sub>2</sub>O<sub>3</sub> film, respectively, indicating that the grain-like structures are clearly observed on top of the Ga<sub>2</sub>O<sub>3</sub> film after the thermal annealing. The root-mean-square (RMS) surface roughnesses of the as-deposited and 1050 °C-annealed Ga<sub>2</sub>O<sub>3</sub> films, respectively, are 0.89 and

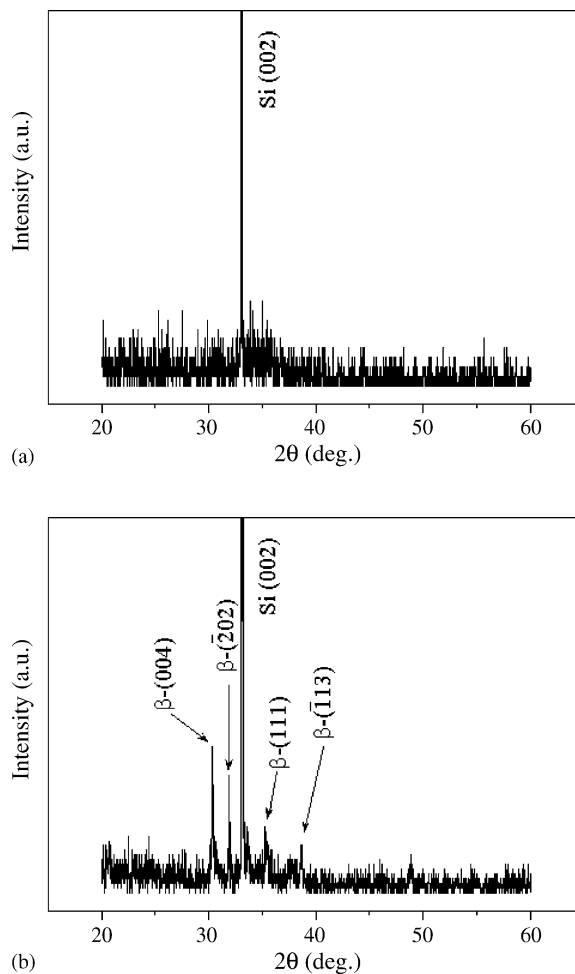


Fig. 4. XRD patterns of the (a) as-deposited and (b) 1050 °C-annealed Ga<sub>2</sub>O<sub>3</sub> thin films.

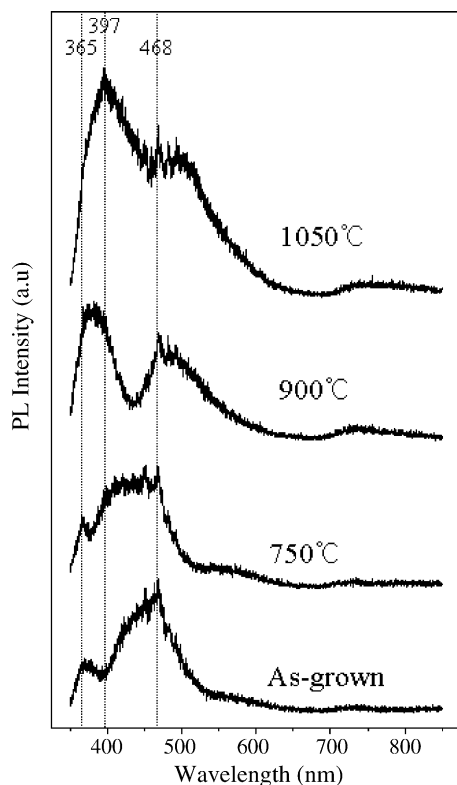


Fig. 5. Room temperature PL spectra of as-deposited and annealed  $\text{Ga}_2\text{O}_3$  films at temperatures in the range of 750–1050 °C.

3.56 nm, indicating that the surface of annealed  $\text{Ga}_2\text{O}_3$  film is more rough than that of the as-deposited  $\text{Ga}_2\text{O}_3$  film. We surmise that the surface becomes rougher due to the appearance of grains on top of the films, and thus the AFM images agree with the SEM images.

In order to investigate the effect of thermal annealing on the crystallinity of  $\text{Ga}_2\text{O}_3$  thin film, we have performed an XRD analysis on the as-deposited and 1050 °C-annealed samples. Fig. 4a shows the XRD diffraction pattern of the as-deposited  $\text{Ga}_2\text{O}_3$  films. Due to the absence of a distinguishable  $\text{Ga}_2\text{O}_3$  diffraction peak, we suppose that the  $\text{Ga}_2\text{O}_3$  films have an amorphous structure. Fig. 4b shows the diffraction pattern of the 1050 °C-annealed  $\text{Ga}_2\text{O}_3$  films, indicating that the lines observed in this diffractogram are found to coincide with (004), ( $\bar{2}$ 02), (111), and ( $\bar{1}$ 13) peak of monoclinic  $\beta\text{-Ga}_2\text{O}_3$  obtained from the Joint Committee on Powder Diffraction Standards (JCPDS) card (No. 43-1012). The stable  $\beta\text{-Ga}_2\text{O}_3$  phase is known to have a monoclinic structure [23]. The existence of the  $\beta\text{-Ga}_2\text{O}_3$  peaks indicates the production of  $\beta\text{-Ga}_2\text{O}_3$  grains on  $\text{SiO}_2$  substrates by the thermal annealing at a sufficiently high temperature.

Fig. 5 shows the PL spectra of as-deposited and annealed  $\text{Ga}_2\text{O}_3$  films in the range of 750–1050 °C, which are recorded at room temperature (300 K). The dominant emissions from as-deposited films are bands located at a wavelength of around 468 nm (2.656 eV) and 365 nm (3.405 eV), respectively, in the blue–green (BG) spectral region and in the ultraviolet (UV) spectral region. UV luminescence of  $\text{Ga}_2\text{O}_3$

has been reported to be attributed to an intrinsic transition, due to the recombination of a self-trapped exciton [24]. PL spectra from the  $\text{Ga}_2\text{O}_3$  films show a strong dependency on the postdeposition annealing. The peak intensity in the UV region shifts to longer wavelengths, which has distinguishable peaks at 397 nm with the annealing at 1050 °C. The peak wavelength change of the PL by the thermal annealing is not clearly understood at this time.

Postdeposition annealing also causes dramatic change in PL band, as shown in Fig. 5, indicating that a strong and broad emission in the green light range appears with the thermal annealing at a high temperature of 900–1050 °C. Since the formation of gallium vacancies enhances green emission [25], we surmise that annealing of  $\text{Ga}_2\text{O}_3$  films on  $\text{SiO}_2$  substrates at high temperatures of 900–1050 °C is in favor of the gallium vacancies, contributing to the appearance of green emission. Further systematic study is necessary in order to reveal the mechanism of the observed emissions.

#### 4. Conclusions

We have prepared the  $\text{Ga}_2\text{O}_3$  films on  $\text{SiO}_2$  substrate by a reaction of a TMGa and  $\text{O}_2$  mixture and have investigated the effects of postdeposition annealing. The SEM images indicate that grain-like structures appear by the thermal annealing and the AFM images reveal that the RMS surface roughness increase by the thermal annealing. The XRD data indicate that even though the as-deposited  $\text{Ga}_2\text{O}_3$  films turn out to be amorphous, the  $\beta\text{-Ga}_2\text{O}_3$  phases appear by the thermal annealing. PL spectra of the as-deposited  $\text{Ga}_2\text{O}_3$  films reveal the dominant emission in the BG and UV regions. Annealing at higher temperature results in the shift of UV band to the longer wavelength region and appearance of a broad green emission band, in addition to the existing BG emission band.

#### Acknowledgements

This work was supported by grant no. R05-2001-000-00843-0 from the Basic Research Program of the Korea Science and Engineering Foundation.

#### References

- [1] M. Fleischer, H. Meixner, *Sens. Actuators B* 26 (1995) 81–84.
- [2] L.P. Sosman, T. Abritta, O. Nakamura, M.M.F. D'aguaiar Neto, *J. Mater. Sci. Lett.* 14 (1995) 19.
- [3] T. Miyata, T. Nakatani, T. Minami, *J. Lumin.* 87–89 (2000) 1183.
- [4] M. Passlack, E.F. Schubert, W.S. Hobson, M. Hong, N. Moriya, S.N. Chu, K. Konstadinis, J.P. Mannaerts, M.L. Schnoes, G.J. Zyzdik, *J. Appl. Phys.* 77 (1995) 686.
- [5] K.L. Chopra, S. Major, D.K. Pandya, *Thin Solid Films* 102 (1983) 1.

- [6] M. Fleischer, W. Hanrieder, H. Meixner, *Thin Solid Films* 190 (1990) 93.
- [7] M. Fleischer, H. Meixner, *Sens. Actuators B* 5 (1991) 115.
- [8] F. Reti, M. Fleischer, H. Meixner, J. Giber, *Sens. Actuators B* 18–19 (1994) 573.
- [9] T. Harwig, J. Schoonman, *J. Solid State Chem.* 23 (1978) 205.
- [10] Y. Li, A. Trinchi, W. Wlodarski, K. Galatsis, K. Kalantar-zadeh, *Sens. Actuators B* 93 (2003) 431.
- [11] A.C. Lang, M. Fleischer, H. Meixner, *Sens. Actuators B* 66 (2000) 80.
- [12] P.P. Macri, S. Enzo, G. Sberveglieri, S. Groppelli, C. Perego, *Appl. Surf. Sci.* 65/66 (1993) 277.
- [13] M. Ogita, K. Higo, Y. Nakanishi, Y. Hatanaka, *Appl. Surf. Sci.* 175/176 (2000) 721.
- [14] M. Orita, H. Hiramatsu, H. Ohta, M. Hirano, H. Hosono, *Thin Solid Films* 411 (2002) 134.
- [15] C. Huang, A. Ludviksson, R.M. Martin, *Surf. Sci.* 265 (1992) 314.
- [16] R. Franchy, M. Eumann, G. Schmitz, *Surf. Sci.* 470 (2001) 337.
- [17] R. Franchy, *Surf. Sci. Rep.* 38 (2000) 195.
- [18] P. Chen, R. Zhang, X.F. Xu, Y.G. Zhou, Z.Z. Chen, S.Y. Xie, W.P. Li, Y.D. Zhang, *Appl. Phys. A* 71 (2000) 191.
- [19] G.A. Battiston, R. Gerbasi, M. Porchia, R. Bertinello, F. Caccavale, *Thin Solid Films* 279 (1996) 115.
- [20] L. Miinea, S. Suh, S.G. Bott, J.-R. Liu, W.-K. Chu, D.M. Hoffman, *J. Mater. Chem.* 9 (1999) 929.
- [21] M. Valet, D.M. Hoffman, *Chem. Mater.* 13 (2001) 2135.
- [22] D.H. Kim, S.H. Yoo, T.-M. Chung, K.-S. An, H.-S. Yoo, Y. Kim, *Bull. Korean Chem. Soc.* 23 (2002) 225.
- [23] Y. Jeliazova, R. Franchy, *Surf. Sci.* 527 (2003) 57.
- [24] E.G. Villora, K. Hatanaka, H. Odaka, T. Sugawara, T. Miura, H. Fukumura, T. Fukuda, *Solid State Commun.* 127 (2003) 385.
- [25] T. Harwig, G.J. Wubs, G.J. Dirksen, *Solid State Commun.* 18 (1976) 1223.